Compact all-optical bypass–exchange switch

Dan M. Marom and David Mendlovic

An electronically or optically addressed compact optical bypass–exchange switch is investigated and experimentally demonstrated. The switch is polarization based and consists of a controllable $\lambda/2$ plate sandwiched between two polarizing beam displacers. The input and the output signals propagate normal to the switching array, which makes the switch extremely attractive for cascading switching arrays, as found in multistage interconnect networks. A complete, all-optical interconnection network is suggested.

Key words: Bypass–exchange switch, optical interconnects, multistage interconnection network.
© 1996 Optical Society of America

1. Introduction

The advantages of optical interconnects have been reviewed in the past,[1,2] promising high bandwidth, low cross talk, and highly parallel communication channels. Although many static optical interconnects have been performed that implement optical waveguides,[3] imaging systems,[4] and holographic optical elements,[5] dynamic optical interconnects pose a greater challenge. A dynamic network is capable of connecting source points to different target points by an addressable agent. One group of networks capable of performing dynamic interconnections is called multistage interconnection networks[6,7] (MIN's). The structure of a MIN is of alternating layers of static interconnection patterns (mathematical mappings such as the perfect shuffle[8]), followed by an array of basic switching modules, known as bypass–exchange switches. The bypass–exchange switch has two inputs and two outputs with two operating modes: bypass, in which input signals and output signals are similar, and exchange, in which input signals are swapped.

There are two basically different ways of performing the elementary bypass–exchange switch for optical signals that propagate in free space. The first switch is a hybrid optoelectronic semiconductor system that employs two photodetectors, basic electronic circuitry for switching, and two lasers or optical modulators. Optical signals are converted to electric current, which, after amplification and electronic switching, are used to drive the two lasers. The efficiency of this process is low, suffers from a reduced signal-to-noise ratio (SNR) owing to noise factors that are introduced, and is confined to subgigabit modulation rates. An all-optical switch performs the switching function without converting the signals from the optical domain to the electronic domain and vice versa. Polarization-based switching first combines the two signals when they are polarized linearly and perpendicularly to each other. The switching itself is done by an exchange of the polarization state of the two signals. Combining and splitting of the two perpendicularly polarized signals have been demonstrated with polarized beam splitters,[9] proposed with Wollaston prisms,[2] and recently demonstrated with a birefringent computer-generated hologram.[10] In this paper the utilization of a polarizing beam displacer is presented, which results in a compact, inexpensive switch that is most appropriate for multistage networks.

A brief presentation of the basic structure of the proposed bypass–exchange switch is given in Section 2. The switch is evaluated with various controllable $\lambda/2$ elements in Section 3, and signal degeneration and cross talk is analyzed. Section 4 is devoted to system performance and to the compactness of the switch, as this feature makes the proposed switch superior to other configurations. An implementation of the bypass–exchange switch in an all-optical MIN is suggested in Section 5.

2. Polarization-Based Bypass–Exchange Switch

The bypass–exchange switch is an elementary switch for a two-input signal and a two-output signal.[11]
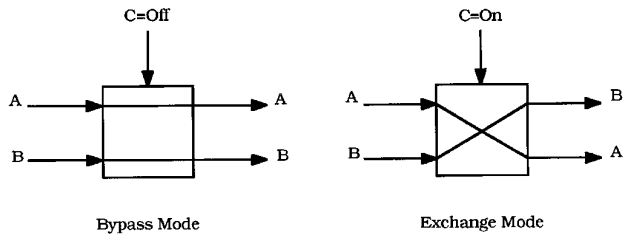
Fig. 1. Schematic representation of a bypass–exchange switch in the two operating modes.

BDP - Beam Displacing Prism (calcite crystal)
↑,⊗ - Polarization Directions

Fig. 3. Optical setup of a bypass–exchange switch. Input and output signals are parallel and in a consistent polarization state, making cascadability feasible.

An additional control-line signal determines whether the two signals pass through unaffected (bypass mode) or are crossed in exchange mode (see schematic representation in Fig. 1).

Optical implementation of the polarization-based bypass–exchange switch requires combination of two optical signals when they are linearly polarized and perpendicular with respect to each other. We propose to take advantage of the phenomenon of double refraction in a crystal of calcite. Calcite, which chemically is calcium carbonate $(CaCO_3)$, occurs in nature in a great variety of crystal forms and is found to be transparent to visible light. When a beam of ordinary unpolarized light is incident upon a calcite crystal, there are two refracted beams and hence double refraction. The ray for which Snell's law is obeyed is called the ordinary ray, and the other is the extraordinary ray. When the faces of a calcite crystal are parallel, the two refracted rays emerge parallel to the incident beam and displaced from each other. If the incident light is normal to the surface, the extraordinary ray is refracted at an angle of 6° and comes out parallel to, but displaced from, the incident beam. The ordinary ray passes straight through without deviation, as seen in Fig. 2. A rotation of the crystal about the ordinary ray, in this case, causes the extraordinary ray to rotate around the fixed ordinary ray.

The optical setup of the bypass–exchange switch is implemented with two calcite beam displacers for combining and splitting two beams, two $\lambda/2$ plates for orienting polarization states in the input and the output, and a controllable $\lambda/2$ device, as illustrated in Fig. 3.

Two adjacent incoming signals, A and B, are assumed to be linearly polarized in the ↑-direction (ordinary) at an earlier stage. Input B propagates through a fixed $\lambda/2$ plate and is converted to a linear polarization in the ⊗-direction (extraordinary). Both signals are now incident upon a calcite crystal, with signal directions (↑ and ⊗) aligned with the crystal's orientation (ordinary and extraordinary).
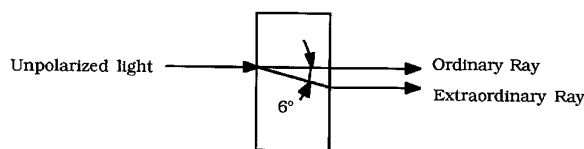
The crystal length provides a displacement that equals the distance between inputs A and B, which guarantees that both signals emerge as one ray with two orthogonal polarizations that represent signals A and B. The signal couple passes through a controllable $\lambda/2$ device, which by a control signal is either active or passive. If the device is active, the two orthogonal polarizations undergo a 90° rotation, with signals A and B exchanging their polarization states. The signal couple is then split up by the second calcite crystal, and the polarization of the ⊗-direction is converted back to the ↑-direction with another fixed $\lambda/2$ plate. The output polarization state is returned to the ↑-direction for consistency with the input polarization state, as the switch is employed in a multistage system.

3. Experimental Results

The experiment described was carried out several times with different devices incorporated for the controllable $\lambda/2$ plate in the setup illustrated in Fig. 3. Each device is evaluated based on performance and implementation feasibility in a large switching array structure. Two circular-aperture signals, 2 mm in diameter and set at a pitch of 2.7 mm, were used to simulate the two input signals. The signal pitch corresponded to the displacement obtained from a calcite crystal of length 24 mm. The two output signals were analyzed with a beam scanner[12] that gave the line-spread function of the intensity of two circles and hence two peaks, as seen in Fig. 4.

The first attempt at operating the bypass–exchange switch was with a nematic liquid-crystal television (LCTV) panel spatial light modulator manu-

Fig. 2. Double refraction of light in a calcite crystal.
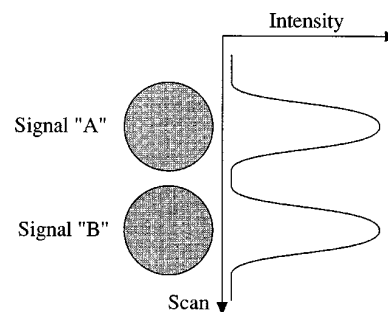
Fig. 4. Measurement method of output obtained by a line-spread function of the two circular signals.

factured by Epson.[13] The LCTV proved insufficient because the maximum polarization rotation angle that was achieved was 55°. We resolved the problem by cascading two LCTV's and by setting proper driving voltages so that the combined rotation angle was 90°. The output signal was very weak because the signal pattern (a circle 2 mm in diameter) was much larger than the pixel size (~80 μm) of the LCTV and suffered from diffraction losses from both panels. The inadequate polarization rotation angle was disappointing because LCTV spatial light modulators are common, relatively inexpensive, and provide dense pixel arrays. However, other LCTV panels might fulfill the requirements of the suggested system.

The second experiment was carried out with a smectic, surface-stabilized ferroelectric liquid-crystal (SSFLC) cell. The cell consists of two glass plates that are covered with transparent electrodes and placed with a small gap between them in which the smectic liquid crystal (LC) lies. The ferroelectric liquid-crystal (FLC) cells are binary in nature and thus have only two functional modes for positive/negative applied voltage. FLC therefore is more attractive than devices based on nematic LC, whose functional characteristic is a function of the applied voltage. The voltage determines only the switching rate with FLC devices. The transmitted light through the cell is given by

$$T = \sin^2(4\theta)\sin^2[\pi\Delta n(\lambda)d/\lambda]. \qquad (1)$$

When $\Delta n(\lambda)d$ equals $\lambda/2$, the cell acts as a half-wave switchable plate [$\Delta n(\lambda)$ is the birefringence of the FLC material, and d is the width of the FLC layer]. For best performance the tilt angle θ of the smectic phase is required to be close to 22.5°. The birefringence [$\Delta n(\lambda)$] of the smectic LC is relatively sensitive to temperature variations; therefore thermal control is an issue that needs addressing.

The experimental results of the bypass–exchange switch are shown in Figs. 5–7. The two signals (circular apertures) resemble peaks when the line-spread function is recorded. Figure 5 displays both signals in the bypass mode and in the exchange mode (linear scale). For analysis of the cross talk associated with the switch, one signal is removed, and attention is given to the energy that is transferred from the remaining signal to the area of the removed signal. As seen in Fig. 6, there is no noticeable cross talk in the bypass and the exchange modes when the signals are observed in linear scale. The cross talk was measured in both modes and was found to be a fraction of 200 (−23 dB) of the signal. The time response of the FLC gate is displayed versus the driving voltage in Fig. 7. At the driving voltage of ±10 V, switching rates were 1 ms. Switching rates for SSFLC are possible in the 10-μs range according to the manufacturer but require higher voltages and thus were not demonstrated. As the FLC is a binary device, the applied voltage affects the switching speed only and therefore does not

(a)

(b)
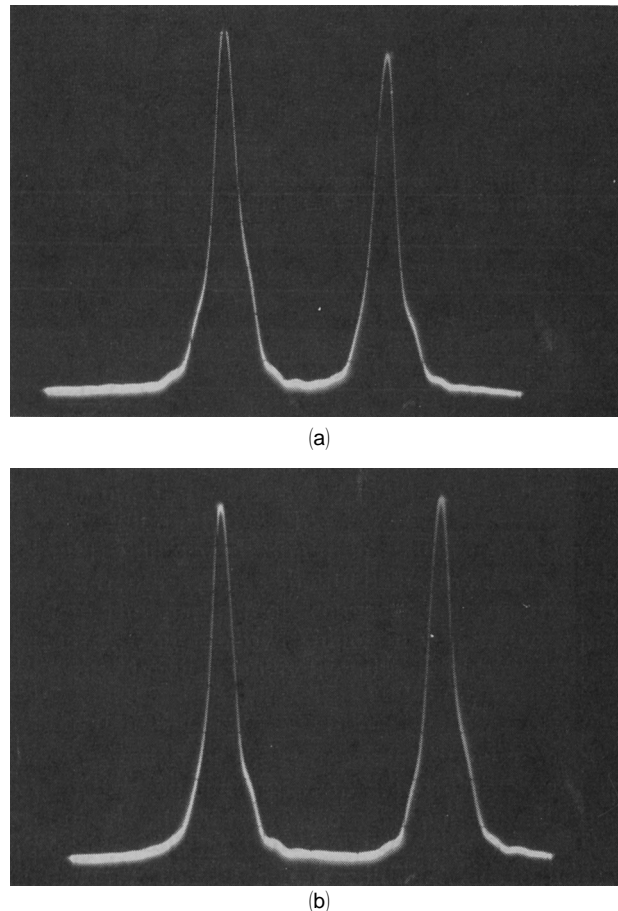
Fig. 5. Output signals in (a) bypass and (b) exchange modes. The peaks are similar, but an observant viewer will note that the two peaks are in exchanged positions.

influence the rotation precision. Temperature sensitivity may require that the FLC device be put in a cryogenic cell. By maintaining precise temperature control, one can reduce the cross-talk term even further.

The last experiment was carried out with a Hughes nontwisted liquid-crystal light valve (LCLV). The LCLV differs from the SSFLC in the previous experiment in several ways. The device functions by modulating an incident optical wave that is reflected back by an internal mirror, and the control signal is optical, which illuminates the back side of the device. The device also requires a driving voltage of 20 VAC at 1 kHz. A folded switch design is possible, which saves half of the components of Fig. 3, because the switch is symmetric about the active $\lambda/2$ device. The performance of the LCLV was inferior to that of the SSFLC. The cross-talk term was −20 dB, and the switching rate was slower owing to the inherent limitations of the nematic LC.

4. Discussion

The suggested bypass–exchange switch is based on orthogonal polarization of the two signals and manipulations on these signals. The performance of the switch deteriorates as deviations from ideal
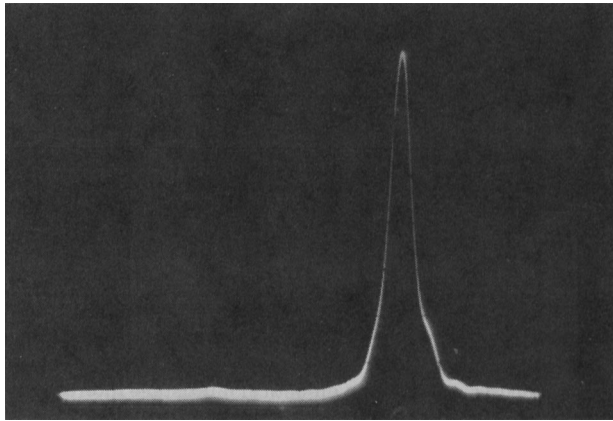
(a)
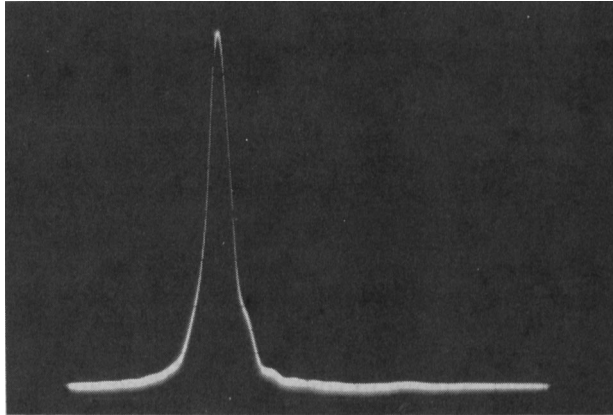
(b)

Fig. 6. Output signals in (a) bypass and (b) exchange modes when only one input signal is present. No cross talk is visible.

assumptions are introduced. As was indicated above, it is presumed that the two signals arrive linearly polarized. If the source of the signals is placed behind a polarizer to attain the desired polarization, then an error coefficient for the polarizer, ϵ_p, can be introduced, which is the extinction
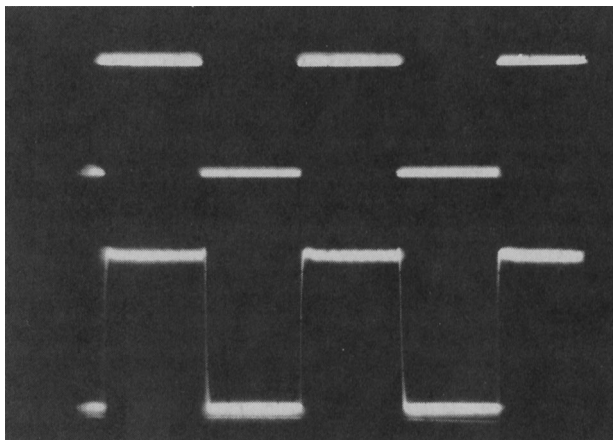
Fig. 7. Output of a single signal as a function of the driving voltage at 10 Hz. Driving voltage is on top; the photodetector reading is on the bottom. As the switching rate increases, delay time becomes noticeable.

ratio. Similarly, error coefficients for the fixed $\lambda/2$ plate, ϵ_f, and for the controllable $\lambda/2$ plate, ϵ_c, are introduced. These error coefficients increase the noise in the system by way of undesirable cross talk. The design of the switch enables simple filtration of the polarization errors that are due to ϵ_p and ϵ_f. Because the calcite crystal combines the correctly polarized signals into one ray, the cross-talk signals (orthogonally polarized) are also combined at a displaced distance from the correct ray (neglecting second-order errors of the form $\epsilon_p\epsilon_f$). This cross-talk signal can be filtered by a simple mask set between the first calcite crystal and the controllable $\lambda/2$ plate without introducing diffraction limitations. The only error coefficient that is left is the one associated with the controllable device, ϵ_c. ϵ_c is assumed to be 1% for a thermally controlled and pixelized SSFLC.

The optical signal attenuation within the entire switch is calculated to be of the order of 4% (ϵ_{att}), assuming a narrowband antireflection coating on all components and some absorption in the controllable device. Attenuation is important for evaluating an all-optical switch, as the switches are used in cascade in multistage systems and optical power is limited. The attenuation of the calcite is insignificant in comparison to reflection losses of the system. This figure could be much lower if several of the components could be integrated. Further research is needed to investigate whether the calcite can replace the glass plates of the SSFLC to reduce the glass–air interfaces.

The overall signal degradation is due to the attenuation and switching loss. The loss per switch is therefore

$$\epsilon = 1 - (1 - \epsilon_{att})(1 - \epsilon_c) \cong 5\%. \tag{2}$$

When the switch is implemented in a MIN, the switching function is carried out by layer after layer of switches. The fractional power in the proper signal channel is

$$S(w) = (1 - \epsilon)^w, \tag{3}$$

where w is equal to the number of switching layers. The signal loss that is due to switching imperfections (ϵ_c error) is energy dissipation to neighboring switches. The power loss is distributed among the other signals in an unknown fashion, owing to the interconnection mapping and the switch setting in the network. The worst-case cross-talk power in an unwanted channel is limited (first-order assumption) by the total energy transfer

$$N(w) = w\epsilon_c. \tag{4}$$

From these two relations the following SNR is deduced, based on cross talk only:

$$\mathrm{SNR} = \frac{S(w)}{N(w)} = \frac{(1 - \epsilon)^w}{w\epsilon_c}. \tag{5}$$

Fig. 8. Plot of the SNR versus the number of stages.
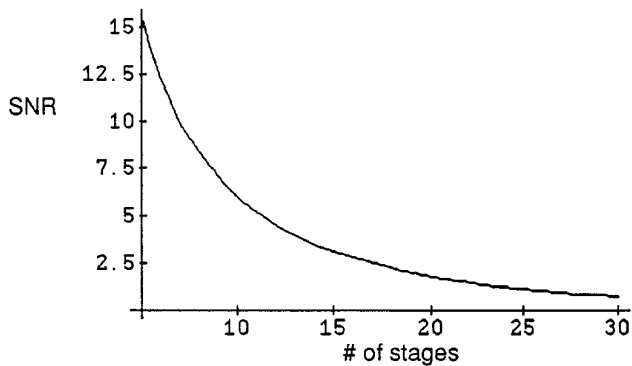
Fig. 9. Proposed setup for an all-optical multistage interconnect network. BDP's, beam-displacing prisms.

The plot of the SNR versus the number of stages is given in Fig. 8. If we assume a minimal SNR of 2 for signals to be properly distinguished, the number of stages can be deduced. Solving for w, with $\epsilon = 5\%$ and $\epsilon_c = 1\%$, the number of levels that can be cascaded is $w = 18$. Although this number is relatively small, it was deduced with strict and conservative assumptions. Even so, with 18 layers of switches, a MIN can permute $N = 512$ inputs, based on $2 \log_2 N$ stages.[14] When the interconnections of the input nodes to the output nodes are carried out with this switch, the optical links are bidirectional; that is, the signals can propagate in the reverse direction simultaneously.

The attractive feature of this bypass–exchange switch is its implementation in a switching array. The density of input signals to an array is double the pixel pitch of the active device because every two signals are combined into one by the beam-displacing prism. The switch can be designed to be very compact by compressing the elements together. For a pixel pitch Δx, each calcite crystal has to be of length $L = \Delta x/(2 \tan 6°) \cong 4.8\Delta x$. If we assume a pixel pitch of 100 µm, then the length of calcite needed is almost 0.5 mm, and the signal pitch is 50 µm. The input and the output signals propagate parallel to each other and perpendicular to the switching array, as opposed to the Wollaston prism arrangement. This facilitates cascading layers of switching arrays for multistage networks. With switching times in the 10-µs range, which is much slower than the bit rate of optical signals, such a switch is suitable for applications that require long interconnection times, as in circuit switching and long packet transmission, with each packet burst lasting at least as long as the reconfiguration time for the process to be efficient.

5. Suggested Setup for an All-Optical Multistage Interconnection Network

Multistage interconnect networks perform arbitrary connections between input and output nodes by setting the different switches to bypass or exchange modes. As noted above, any permutation can be achieved in $2 \log_2 N$ stages of mathematical mappings, such as the perfect shuffle and $N/2$ switches
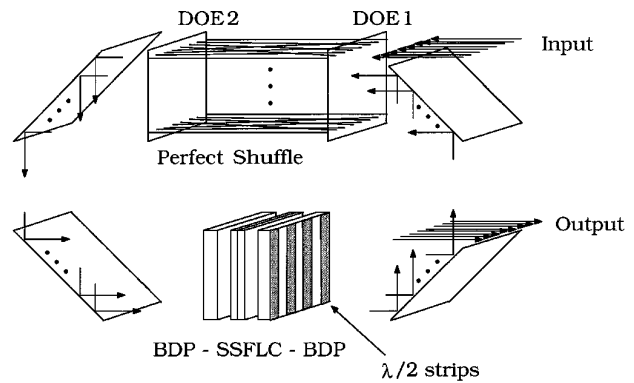
per stage. Therefore, an interconnection system for 16 input/output nodes requires 8 stages and 64 switches.

The mapping can be performed by diffractive optical elements (DOE's) that are space variant[15] or other suggested semi-space-variant schemes.[4,16,17] The perfect shuffle is attractive because the same mapping is utilized in every layer. A suggested layout for the network is therefore in an almost-closed loop (Fig. 9). This layout functions exactly as a planar configuration, only the stages are folded, generating a three-dimensional layout that is compact. Thus, 8 loops in this layout replace an axial extent of 8 stages. The input vector of 16 elements is incident upon the first DOE, which directs each input signal in the vector to its fixed mapping. The second DOE aligns the ray for continued propagation. After passing through the switching array, the signal vector is directed back to the first DOE. By the vector being returned to the first diffractive phase mask, parallel to the input vector but displaced from it, the process is repeated. This closed loop is repeated 8 times, and only on the last run is the output permitted to escape the feedback mirror. Such a setup requires one pixelized dynamic $\lambda/2$ plate, with 8×8 pixels, two DOE's, two calcite crystals, and vertical stripes of fixed $\lambda/2$ plates, for orienting the polarization states in the switch. The system does have a problem because the signals are projected and therefore suffer from divergence. However, one may overcome this problem by keeping short propagation distances and relatively large pixels or by introducing imaging optics in the loop to compensate for diffraction.

6. Conclusions

An all-optical bypass–exchange switch has been demonstrated that uses polarizing beam displacers of calcite crystal. The SSFLC device was found to be most appropriate in comparison to LCTV and LCLV. The advantages are compact switch structure (total added axial length to the SSFLC approximately ten times pixel pitch), electric control, simple large-scale integration in a switching array, high density of signals (twice the pixel pitch in a linear

array), fast reconfiguration time, all-optic switching, and cascadability.

An optical cross talk of -23 dB was measured. Assuming a cross talk of -20 dB in a pixelized array and reflection losses of 4% per switch, one can assemble 18 consecutive layers of switches before the signal is indistinguishable. A switching network can be constructed for 512 inputs for this level of cross talk.

References and Notes

1. J. W. Goodman, F. I. Leonberger, S. Y. Kung, and R. A. Athale, "Optical interconnection for VLSI systems," Proc. IEEE **72,** 850–866 (1984).
2. A. W. Lohmann, "What classical optics can do for the digital optical computer," Appl. Opt. **25,** 1543–1549 (1986).
3. S. Somekh, E. Garmire, A. Yariv, H. L. Garvin, and R. G. Hunsperger, "Channel optical waveguides and directional couplers in GaAs-imbedded and ridged," Appl. Opt. **13,** 327–330 (1974).
4. A. W. Lohmann, W. Stork, and G. Stucke, "Optical perfect shuffle," Appl. Opt. **25,** 1530–1531 (1986).
5. R. K. Kostuk, J. W. Goodman, and L. Hesselink, "Design considerations for holographic optical interconnects," Appl. Opt. **26,** 3947–3953 (1987).
6. C.-L. Wu and T.-Y. Feng, "The universality of the shuffle-exchange network," IEEE Trans. Comput. **C-30,** 324–331 (1981).
7. H. M. Ozaktas and D. Mendlovic, "Multistage optical implementation architecture with least possible growth of system size," Opt. Lett. **18,** 296–298 (1993).
8. H. S. Stone, "Parallel processing with the perfect shuffle," IEEE Trans. Comput. **C-20,** 153–161 (1971).
9. K. M. Johnson, M. R. Surette, and J. Shamir, "Optical interconnection network using polarization-based ferroelectric liquid crystal gates," Appl. Opt. **27,** 1727–1733 (1988).
10. F. Xu, J. E. Ford, and Y. Fainman, "Polarization-selective computer-generated holograms: design, fabrication, and applications," Appl. Opt. **34,** 256–266 (1995).
11. E. Fredkin and T. Toffoli, "Conservative logic," Int. J. Theoret. Phys. **21,** 219–223 (1982).
12. BeamScan, model 1180 GP, by Photon, Inc. The sampling aperture is 25 μm.
13. Crystal Image video projector by Epson. The LCTV panel has 320×220 pixels of pitch 80 μm.
14. T.-Y. Feng and S.-W. Seo, "A new routing algorithm for a class of rearrangeable networks," IEEE Trans. Comput. **43,** 1270–1280 (1994).
15. K. S. Urquhart, P. Marchand, Y. Fainman, and S. H. Lee, "Diffractive optics applied to free-space optical interconnects," Appl. Opt. **33,** 3670–3682 (1994).
16. K.-H. Brenner and A. Huang, "Optical implementation of the perfect shuffle interconnection," Appl. Opt. **27,** 135–137 (1988).
17. K. Noguchi, K. Hogari, T. Sakano, and T. Matsumoto, "Rearrangeable multichannel free-space optical switch using polarization multiplexing technique," Electron. Lett. **26,** 1325–1326 (1990).
18. Fabia Engineering Ltd., Multipurpose Building 3, Kiryat Weizmann Science Park, Ness Ziona 70400, Israel. Fax: 972-8-408085.